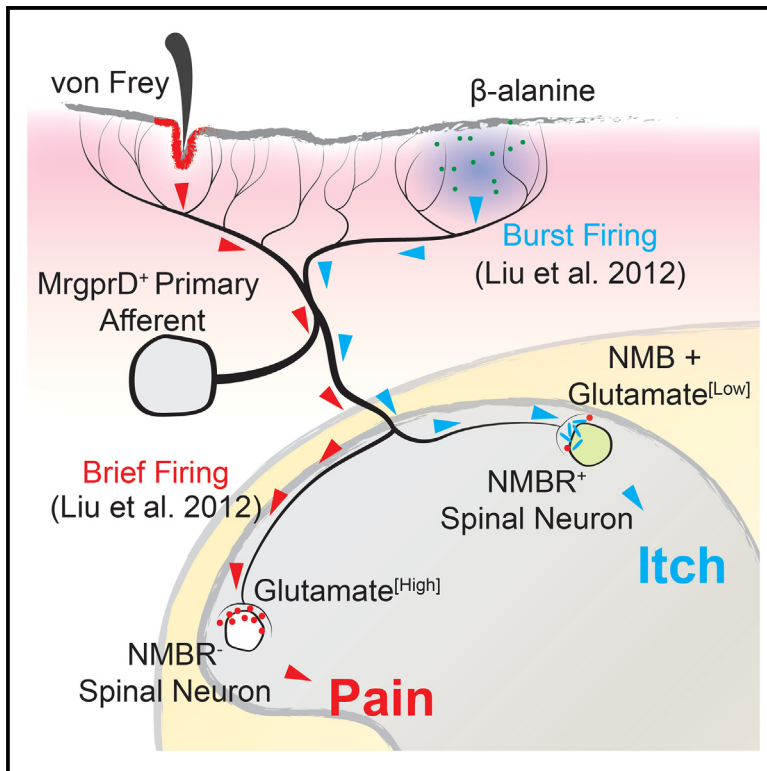


Pain and itch coding mechanisms of polymodal sensory neurons

Graphical abstract



Authors

Changxiong Guo, Haowu Jiang, Cheng-Chiu Huang, ..., George Hoekel, Wenqin Luo, Qin Liu

Correspondence

qinliu@wustl.edu

In brief

Guo et al. identify the pain and itch coding mechanisms of MrgprD⁺ primary afferent neurons. While only glutamate is required for mechanical pain signals mediated by this population, the neuropeptide neuromedin B (NMB) and a subthreshold quantity of glutamate are released together to excite NMB-sensitive postsynaptic circuits for itch signals.

Highlights

- Polymodal MrgprD⁺ primary afferent neurons express *Vglut2* and *Nmb*
- Glutamate is required for both pain and itch signaling from MrgprD⁺ neurons
- NMB is selectively required for itch signaling
- NMBR⁺ central neurons are required for MrgprD⁺-neuron-mediated itch signals



Article

Pain and itch coding mechanisms of polymodal sensory neurons

Changxiong Guo,^{1,3} Haowu Jiang,^{1,3} Cheng-Chiu Huang,¹ Fengxian Li,¹ William Olson,² Weishan Yang,¹ Michael Fleming,² Guang Yu,¹ George Hoekel,¹ Wenqin Luo,² and Qin Liu^{1,4,*}

¹Washington University Pain Center, Department of Anesthesiology, Washington University School of Medicine in St. Louis, St. Louis, MO 63110, USA

²Department of Neuroscience, University of Pennsylvania, Perelman School of Medicine, Philadelphia, PA 19104, USA

³These authors contributed equally

⁴Lead contact

*Correspondence: qinliu@wustl.edu

<https://doi.org/10.1016/j.celrep.2023.113316>

SUMMARY

Pain and itch coding mechanisms in polymodal sensory neurons remain elusive. MrgprD⁺ neurons represent a major polymodal population and mediate both mechanical pain and nonhistaminergic itch. Here, we show that chemogenetic activation of MrgprD⁺ neurons elicited both pain- and itch-related behavior in a dose-dependent manner, revealing an unanticipated compatibility between pain and itch in polymodal neurons. While VGlut2-dependent glutamate release is required for both pain and itch transmission from MrgprD⁺ neurons, the neuropeptide neuromedin B (NMB) is selectively required for itch signaling. Electrophysiological recordings further demonstrated that glutamate synergizes with NMB to excite NMB-sensitive postsynaptic neurons. Ablation of these spinal neurons selectively abolished itch signals from MrgprD⁺ neurons, without affecting pain signals, suggesting a dedicated itch-processing central circuit. These findings reveal distinct neurotransmitters and neural circuit requirements for pain and itch signaling from MrgprD⁺ polymodal sensory neurons, providing new insights on coding and processing of pain and itch.

INTRODUCTION

Pain and itch are unpleasant but distinct sensations. Despite recent progress in the identification and characterization of molecular receptors involved in pain and itch detection,^{1–3} how pain and itch signals are encoded and transmitted from primary sensory neurons to the central nervous system remains contentious. Previous studies have identified several highly restricted populations of primary sensory neurons detecting a particular sensory modality (e.g., TRPM8⁺ neurons for cold, and MrgprA3⁺ neurons for itch).^{4,5} However, most nociceptive afferent neurons are polymodal and can be involved in both pain and itch. How polymodal sensory neurons differentiate and encode pain and itch signals remains unclear.

The expression of MrgprD defines one of the main populations of polymodal sensory neurons in the dorsal root ganglia and trigeminal ganglia.^{6–8} MrgprD is a G protein-coupled receptor identified in both human and mouse sensory neurons.^{9,10} MrgprD-expressing neurons are polymodal C-fiber neurons that mainly innervate the skin¹¹ and can be activated by chemical, mechanical, and thermal stimuli.^{6–8} Studies have shown that MrgprD is selectively activated by β -alanine and mediates nonhistaminergic itch in the skin.^{8,12} In addition, MrgprD⁺ neurons can be activated by punctate mechanical stimuli or pinching and mediate mechanical pain.^{13,14} Although MrgprD⁺-neuron-mediated itch and pain were reported in pre-

vious studies, it is unclear whether MrgprD⁺ neurons produce pain and itch in a mutually exclusive (incompatible) manner and whether the behavioral consequence is determined by stimulus modalities or intensities.

Studies have shown that MrgprD⁺ neurons synapse with most known neuronal classes in the substantia gelatinosa (SG; lamina II) of the spinal cord and brainstem.^{15,16} However, it is unclear which population(s) of SG neurons signal pain or itch and how MrgprD⁺ neurons communicate with these neurons. Our previous *in vivo* electrophysiological recordings showed that firing patterns of MrgprD⁺ neurons are different in response to pain vs. itch stimuli. Specifically, noxious mechanical stimuli induce brief action potential firing in MrgprD⁺ neurons, while itch-inducing β -alanine induces prolonged burst firing.⁸ We hence hypothesize that different patterns of electrical activities lead to different neurotransmitter release and activation of discrete SG neuronal populations and circuits.

In this study, we indeed identified different neurotransmitter requirements for pain and itch transmission from MrgprD⁺ neurons. MrgprD⁺ neurons further synapse with segregated populations of central neurons that independently process pain and itch. These results reveal differential mechanisms in coding and transmission of pain and itch signaling in MrgprD⁺ polymodal sensory neurons, complementing previous studies of itch-selective populations.^{2–4,17}



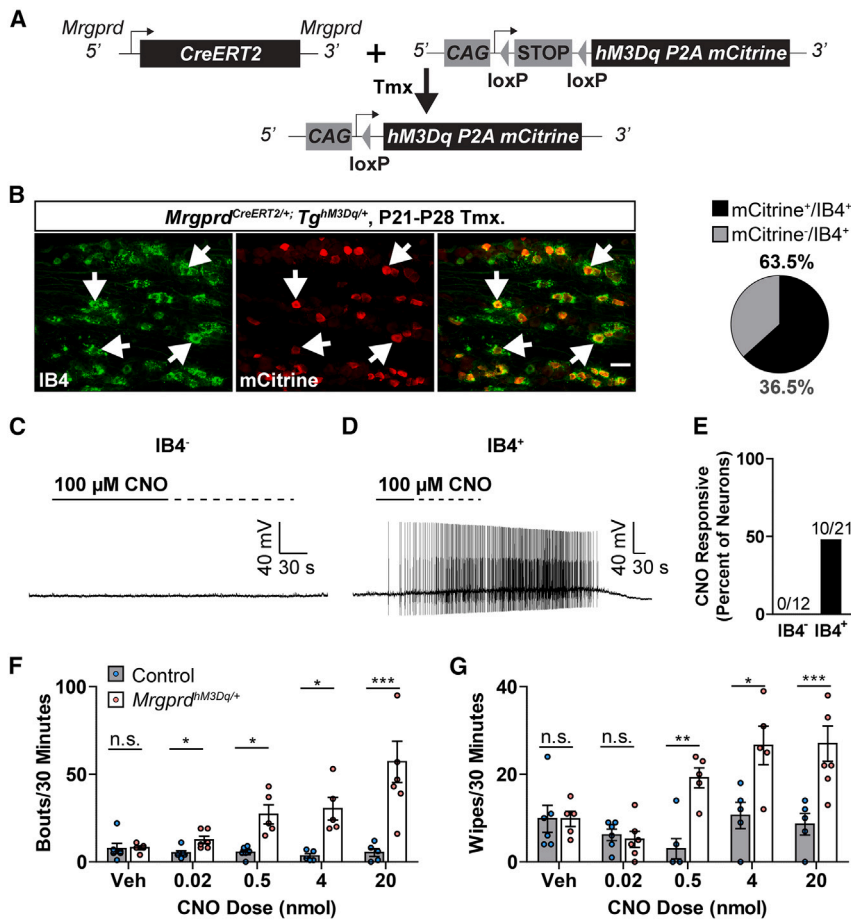


Figure 1. Chemogenetic activation of MrgprD⁺ sensory neurons produces both pain and itch behavioral responses

(A) Breeding strategy for the generation of *Mrgprd^{hM3Dq/+}* mice. *Mrgprd^{CreERT2/+}* are crossed with *Tg^{CAG-hM3Dq/+}* mice to produce *Mrgprd^{CreERT2/+}; Tg^{CAG-hM3Dq/+}* (*Mrgprd^{hM3Dq/+}*) mice and control littermates. After tamoxifen-induced cre recombination, the floxed stop codon between the *hM3Dq* allele and CAG promoter is excised in MrgprD-expressing cells. (B) Immunofluorescence staining showed that 63.5% of IB4⁺ sensory neurons express mCititrine. Arrows indicate mCititrine⁺ neurons (n = 3 mice). Findings were confirmed by RNAscope. See also Figure S1.

(C and D) Whole-cell current-clamp recordings of cultured IB4⁻ (C) and IB4⁺ (D) DRG neurons from *Mrgprd^{hM3Dq/+}* mice. Traces are representative of neuronal responses to CNO stimulation (0.1 mM, bath applied).

(E) Quantification of CNO responses in cultured DRG from *Mrgprd^{hM3Dq/+}* mice (n ≥ 12 neurons per group, from 4 mice).

(F and G) Intradermal cheek injections of CNO produced simultaneous pain and itch responses in *Mrgprd^{hM3Dq/+}* mice. When injected into the cheek (20 μL, in 1% DMSO in saline vehicle), CNO robustly induced scratching (F) and wiping (G) in a dose-dependent manner (n ≥ 5 mice per genotype per dose). Please note that the vehicle control induced mild pain-related wiping behavior in both control and *Mrgprd^{hM3Dq/+}* mice, which may mask pain responses at the lowest tested CNO dose.

Data are presented as mean ± SEM. Nonparametric Mann-Whitney U tests were used to determine statistical significance for (F) and (G). n.s., no significance. *p ≤ 0.05, **p ≤ 0.01, ***p ≤ 0.001. Scale bars: 50 μm.

RESULTS

Chemogenetic activation of MrgprD⁺ sensory neurons produces both pain and itch behavioral responses

Studies have shown that mechanical activation of MrgprD⁺ neurons generates pain,^{13,14} whereas chemical activation of MrgprD⁺ neurons by β-alanine evokes nonhistaminergic itch.⁸ However, it is unclear whether these distinct behavioral consequences are determined by stimulus modalities or intensities and whether pain and itch are produced in a mutually exclusive (incompatible) manner. To address these questions, we tested whether a single stimulus for MrgprD⁺ neurons can generate both pain and itch compatibly using the approach of designer receptors exclusively activated by designer drugs (DREADD). By crossing *Mrgprd^{CreERT2/+}* mice¹⁵ with Cre-dependent *Tg^{CAG-LSL-hM3Dq-mCititrine}* mice, we generated *Mrgprd^{CreERT2/+}; Tg^{CAG-LSL-hM3Dq-mCititrine}* chemogenetic mice (Figure 1A). In this line, the engineered Gq-coupled DREADD receptor hM3Dq and mCititrine reporter are expressed in MrgprD⁺ neurons after tamoxifen-induced CreERT2 nuclear translocation and DNA recombination (referred to as *Mrgprd^{hM3Dq/+}*). Immunofluorescence staining showed that 63.5% of IB4⁺ sensory neurons ex-

press the mCititrine reporter in *Mrgprd^{hM3Dq/+}* mice (Figure 1B). This percentage is consistent with the proportion of IB4⁺ neurons that express MrgprD.^{9,11} Further RNAscope *in situ* hybridization confirmed the co-localization of *hM3Dq* and *Mrgprd* mRNA expression in *Mrgprd^{hM3Dq/+}* mice (Figure S1). Whole-cell patch-clamp recordings show that CNO excited a subset of IB4⁺ sensory neurons from *Mrgprd^{hM3Dq/+}* mice but not control mice (Figures 1C–1E), demonstrating the functional expression of hM3Dq in MrgprD⁺ neurons.

To study the behavioral consequence of chemogenetic activation of MrgprD⁺ neurons, we injected CNO into the cheek skin of *Mrgprd^{hM3Dq/+}* mice. Study has shown that pain induces wiping behavior, whereas itch induces scratching behavior, in mice.¹⁸ Interestingly, CNO induced both pain-related wiping behavior and itch-related scratching behavior in *Mrgprd^{hM3Dq/+}* mice but not control mice (Figures 1F and 1G). Importantly, both wiping and scratching increased with CNO doses (Figures 1F and 1G), with no indication of cross inhibition between pain and itch mediated by MrgprD⁺ neurons. These results, for the first time, reveal that pain and itch can be induced in a compatible manner by a single stimulus for MrgprD⁺ polymodal sensory neurons.

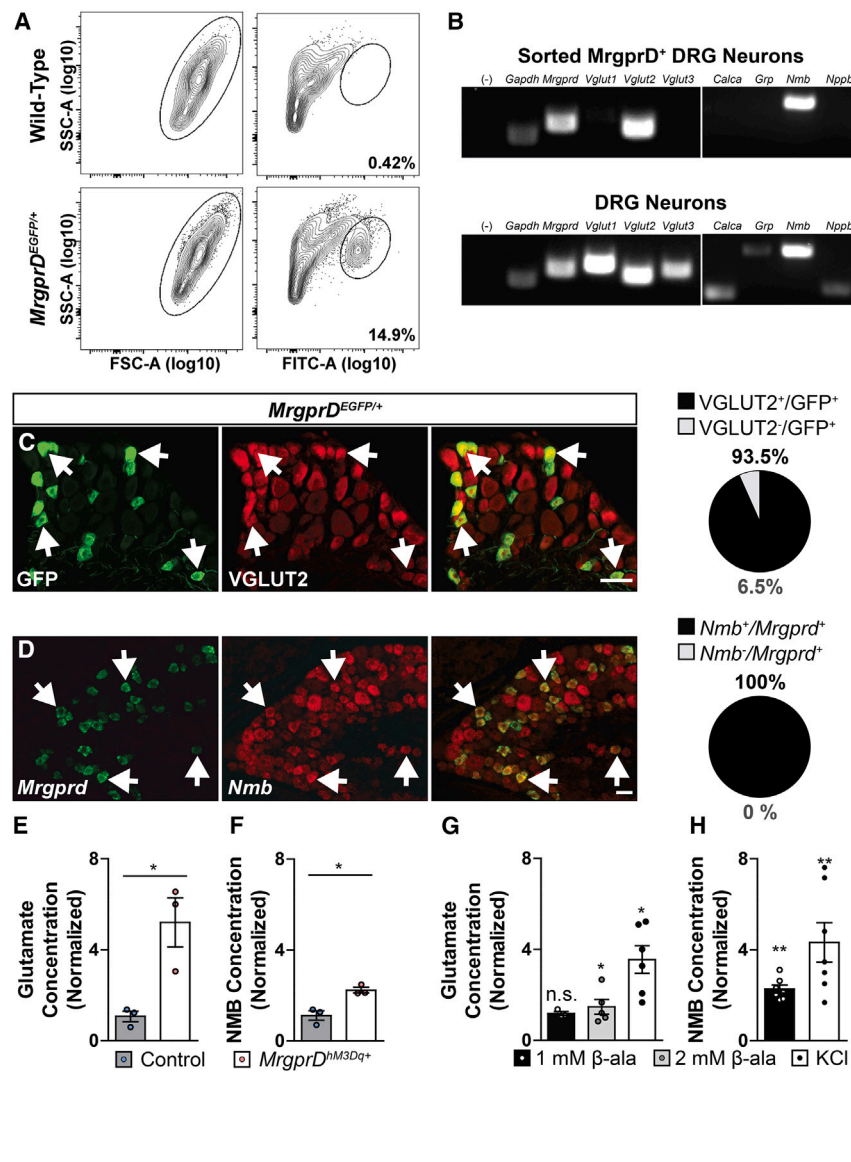


Figure 2. Glutamate and neuromedin B (NMB) are released by *MrgprD*⁺ neurons for synaptic transmission

(A) Fluorescence-activated cell sorting (FACS) analysis of GFP⁺ neurons from *wild-type* and *MrgprD*^{EGFP/+} mice. Gated GFP⁺ fraction accounted for ~15% of all events.

(B) RT-PCR analysis of solute vesicle and neurotransmitter precursor expression in FACS-purified *MrgprD*-GFP neurons. The glutamate transporters *Vglut1* and *Vglut3* and the neuropeptides *Cgrp*, *Grp*, and *Nppb* were not detected in *MrgprD*-GFP neurons, while *Vglut2* and *Nmb* were robustly expressed by this population. BSA-purified, unsorted DRG neurons were used as a control.

(C) Immunofluorescence staining of DRGs from *MrgprD*^{EGFP/+} mice showed broad co-expression of VGLUT2 in GFP⁺ neurons, indicating that most *MrgprD*⁺ neurons expressed VGLUT2 (n = 3 mice).

(D) *In situ* analysis showed that all *MrgprD*⁺ neurons expressed *Nmb* (n = 3 mice).

(E) Extracellular glutamate level of cultured DRG neurons from control and *MrgprD*^{hM3Dq/+} mice after vehicle or CNO treatment (500 μ M), as determined by enzymatic assay. Data are normalized to vehicle treatment (n = 3 biological pairs).

(F) Extracellular NMB level of cultured DRG neurons from control and *MrgprD*^{hM3Dq/+} mice after vehicle or CNO treatment, as determined by ELISA (n = 3 biological pairs).

(G) Extracellular glutamate level of cultured DRG neurons from wild-type mice after β -alanine (1 or 2 mM, as indicated) or KCl (30 mM) treatment. Data are normalized to vehicle treatment. Mean value is indicated above each column (n \geq 5 biological replicates).

(H) Extracellular NMB level of cultured DRG neurons from wild-type mice after vehicle, β -alanine (1 mM), or KCl (30 mM) treatment. Data are normalized to vehicle treatment. (n = 7 biological replicates).

All data are presented as mean \pm SEM. Shapiro-Wilk tests were used to determine data normality for (E)–(H). Unpaired Student's t tests were used to determine statistical significance for (E) and (F). Paired (pre/post) Student's t tests were used for (G) and (H). *p \leq 0.05, **p \leq 0.01. Scale bars: 50 μ m.

MrgprD⁺ sensory neurons express both the vesicular glutamate transporter 2 and neuropeptide neuromedin B

Our chemogenetic results raised the question of how pain and itch signals from *MrgprD*⁺ neurons are transmitted to and deciphered by central neurons. RT-PCR of sorted *MrgprD*-EGFP neurons from *MrgprD*^{EGFP/+} mice indicate that *MrgprD*⁺ neurons selectively express the vesicular glutamate transporter 2 (*Vglut2*), which transports glutamate into synaptic vesicles,¹⁹ and the neuropeptide neuromedin B (*Nmb*) (Figures 2A and 2B). In contrast, the pain- or itch-related neuropeptides CGRP (*Calca*), gastrin-releasing peptide (*Grp*), and natriuretic peptide B (*Nppb*) were not detected in *MrgprD*⁺ neurons (Figure 2B). Further immunostaining and *in situ* hybridization confirm that *Vglut2* is expressed by most *MrgprD*-EGFP neurons (230/246; Figure 2C), and *Nmb* mRNA was present in all

MrgprD⁺ neurons (962/962; Figure 2D). Since chemogenetic activations of *MrgprD*⁺ neurons evoke both pain and itch, we tested whether glutamate and NMB are released by *MrgprD*⁺ neurons for pain and itch signaling. CNO treatments of cultured sensory neurons from *MrgprD*^{hM3Dq/+} mice resulted in significant release of both glutamate and NMB peptide, which was not detected in control mice (Figures 2E and 2F). Compared with CNO, the itch-inducing *MrgprD* agonist β -alanine elicited significant release of NMB, albeit mild glutamate release, from dorsal root ganglion (DRG) neurons of wild-type (WT) mice (Figures 2G and 2H). Taken together, our data show that *MrgprD*⁺ neurons express *Vglut2* and *Nmb* and release glutamate and NMB peptide upon chemogenetic activation. Pruritogen challenge likely induces the release of peptide NMB preferentially, accompanied by low glutamate co-release, from *MrgprD*⁺ neurons.

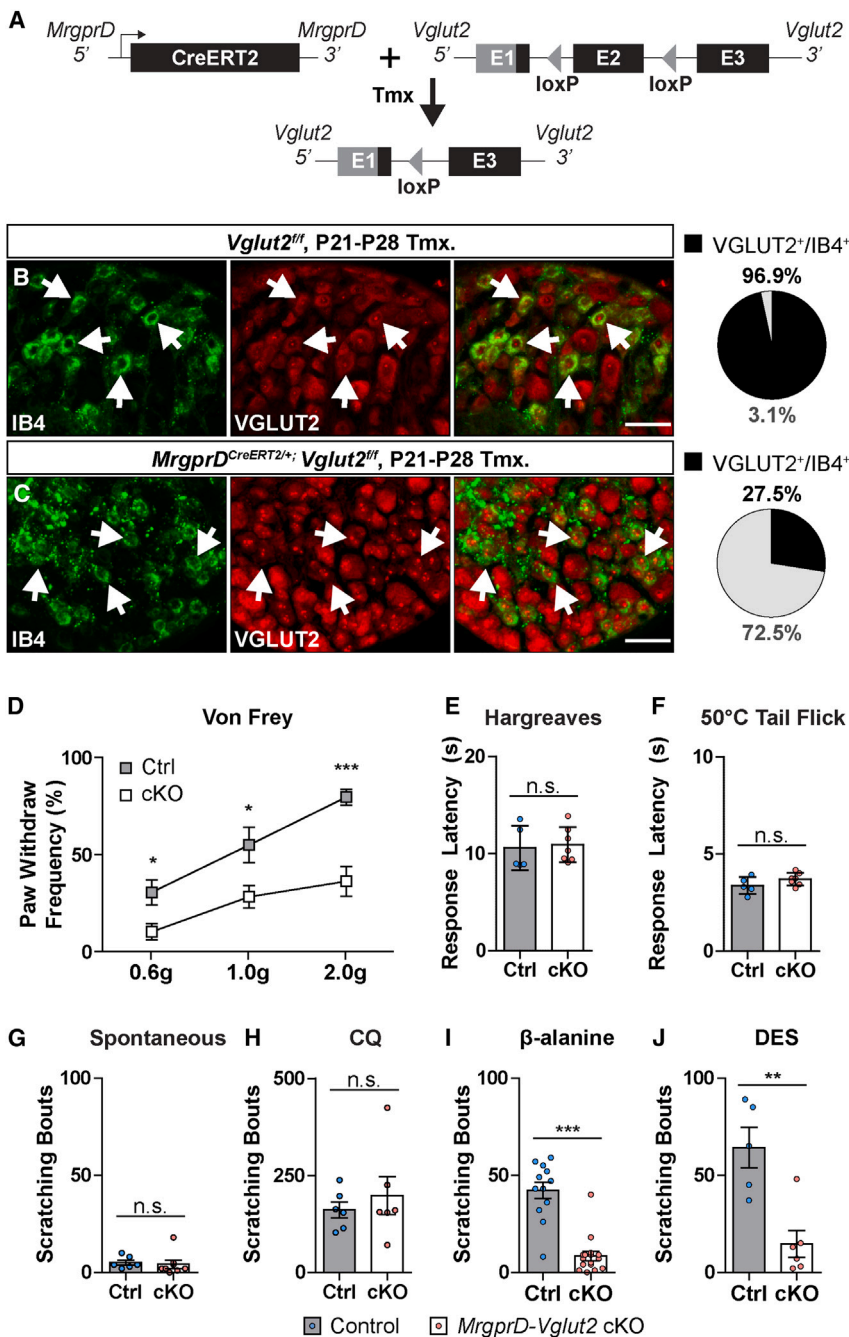


Figure 3. Glutamate is required for signal coding and transmission of both pain and itch in *MrgprD*⁺ sensory neurons

(A) Breeding strategy for the generation of *MrgprD-Vglut2* cKO mice. After tamoxifen-induced Cre recombination, the floxed exon 2 of *Vglut2* is excised in *MrgprD*-expressing cells, resulting in the conditional deletion of VGLUT2 in *MrgprD*⁺ cells. Note, the deletion of exon 2 produces a reading frameshift; no subsequent exon is translated in *Vglut2*.

(B and C) Immunofluorescence staining of VGLUT2 in DRGs from control and *MrgprD-Vglut2* cKO mice. After tamoxifen-induced recombination, VGLUT2 expression was reduced from 96.9% IB4⁺ trigeminal ganglia (TG) and DRG neurons in control mice (B) to only 27.5% in *MrgprD-Vglut2* cKO mice (C) (n ≥ 3 mice per genotype). See also Figure S2.

(D–J) *MrgprD-Vglut2* cKO mice showed defects in mechanical pain and nonhistaminergic itch. (D) *MrgprD-Vglut2* cKO mice exhibited significantly lower sensitivity to noxious mechanical stimuli (n = 10 per group). (E and F) *MrgprD-Vglut2* cKO mice did not show defects in thermal nociception, as measured by (E) Hargreaves assay (n ≥ 5 per group) and (F) tail flick assay (50°C, n ≥ 5 per group). (G and H) *MrgprD-Vglut2* cKO mice did not develop (G) spontaneous itch (n = 8 per group) or (H) enhanced itch responses to chloroquine (0.16 μmol in 20 μL, n = 6 per group). In contrast, (I) β-alanine- (1 μmol) and (J) diethylstilbestrol (DES; 1 μmol in 50 μL ethanol vehicle for topical nape application)-induced scratching were significantly reduced (n ≥ 12 and n = 6 per genotype, respectively). Unless otherwise indicated, all injections were 20 μL at the cheek using saline vehicle. Itch behavior was recorded and analyzed for 15 min, except for the chloroquine assay (30 min).

Data are presented as mean ± SEM. Nonparametric Mann-Whitney U tests were used to determine statistical significance for (D)–(J). n.s., no significance. *p ≤ 0.05, **p ≤ 0.01, ***p ≤ 0.001. Scale bars: 50 μm.

littermate controls to only 27.5% IB4⁺ neurons in *MrgprD-Vglut2* cKO mice (Figures 3B and 3C). The ~70% decrease in VGLUT2/IB4 co-localization is consistent with the proportion of *MrgprD*-expressing neurons within the IB4⁺ population.^{9,11}

Notably, the expression of the other two vesicular glutamate transporters (*Vglut1*

and *Vglut3*) remains undetectable in *MrgprD*⁺ neurons after the genetic deletion of *Vglut2* (Figure S2), arguing against potential compensatory mechanisms by VGLUT1 or VGLUT3.

Next, we tested whether VGLUT2-dependent glutamate release is required for nociceptive signaling from *MrgprD*⁺ neurons. *MrgprD-Vglut2* cKO mice exhibited significantly reduced paw withdrawal frequencies to von Frey stimulation at all tested forces (from 0.6 to 2.0 g; Figure 3D), indicating that they are less sensitive to noxious mechanical stimuli. In contrast, no differences in thermal pain responses were observed between

VGLUT2-dependent glutamate release is required for signal coding and transmission of both pain and itch in *MrgprD*⁺ sensory neurons

To determine the role of glutamate in pain and itch signaling from *MrgprD*⁺ neurons, we generated *MrgprD^{CreERT2/+}; Vglut2^{F/F}* mice in which *Vglut2* was conditionally deleted from *MrgprD*⁺ neurons after postnatal tamoxifen treatment (referred to as *MrgprD-Vglut2* conditional knockout [cKO] mice; Figure 3A). Immunostaining confirmed that VGLUT2 expression was decreased from 96.9% IB4⁺ neurons in

Mrgprd-Vglut2 cKO and controls in Hargreaves or tail flick assays (Figures 3E and 3F), correlating well with previous studies showing the normal thermal sensitivity of *Mrgprd*⁺-neuron-ablated mice.^{13,20} These results demonstrate that VGlut2-dependent synaptic glutamate release from *Mrgprd*⁺ neurons is required for signaling mechanical pain.

Previous studies have shown that cKO of *Vglut2* in Nav1.8- or TRPV1-lineage neurons (including *Mrgprd*⁺ neurons and many other small-diameter sensory neurons²¹) leads to enhancement of acute itch and even spontaneous itch in older mice.^{22,23} This effect is thought to be attributed to the interruption of tonic suppression of itch by pain at the circuit level. However, *Mrgprd-Vglut2* cKO mice did not display spontaneous itch even 4 months after tamoxifen treatment (Figure 3G). Furthermore, *Mrgprd-Vglut2* cKO mice did not show enhanced acute itch to chloroquine (an itch-inducing compound that activates an *Mrgprd*-independent population²⁴) (Figure 3H). These results indicate that the mechanical pain defects of *Mrgprd-Vglut2* cKO mice do not impair tonic suppression of itch or enhance itch at the circuit level.

In contrast to the finding that VGlut2-dependent glutamate signal is dispensable for itch signaling,^{22,23} *Mrgprd*⁺-neuron-mediated itch was nearly abolished in *Mrgprd-Vglut2* cKO mice. Scratching responses to β -alanine were significantly attenuated in *Mrgprd-Vglut2* cKO mice compared with control littermates (Figure 3I). In addition, itch responses to topically applied diethylstilbestrol (DES), a synthetic nonsteroidal estrogen that directly activates both human and mouse *Mrgprd* receptors,²⁵ was also reduced in *Mrgprd-Vglut2* cKO mice (Figure 3J). These results demonstrated that glutamate is required for coding and transmitting both pain and itch signals from *Mrgprd*⁺ neurons.

Neuropeptide NMB is selectively required for itch sensation in *Mrgprd*⁺ neurons

The indispensable roles of glutamate in both pain and itch signaling raise the question of how pain and itch signals from *Mrgprd*⁺ neurons are differentiated by central neurons. Besides glutamate, NMB is expressed by *Mrgprd*⁺ neurons. To determine the role of NMB in signaling pain and itch in *Mrgprd*⁺ neurons, we generated *Mrgprd*^{CreERT2/+};*Nmb*^{F/F} mice (referred to as *Mrgprd-Nmb* cKO mice after tamoxifen induction; Figure 4A). Single-cell RT-PCR confirmed that *Nmb* was specifically deleted from *Mrgprd*⁺ neurons of *Mrgprd-Nmb* cKO mice (Figures 4B and 4C). Compared with their littermate controls, *Mrgprd-Nmb* cKO mice displayed normal paw withdrawal responses to von Frey stimulation at all tested forces (Figure 4D), suggesting that NMB is not required for mechanical pain signaling from *Mrgprd*⁺ neurons. Likewise, no defects were found in their thermal pain responses in Hargreaves and tail flick assays (Figures 4E and 4F). In contrast, itch responses to intradermal injection of β -alanine were nearly abolished in *Mrgprd-Nmb* cKO mice compared with control littermates (Figure 4G). Moreover, scratching behavior induced by topically applied DES was significantly attenuated in *Mrgprd-Nmb* cKO mice (Figure 4H). These results indicate that NMB is required for signaling itch rather than mechanical pain mediated by *Mrgprd*⁺ neurons.

To confirm the selectivity of NMB for itch signaling in *Mrgprd*⁺ neurons, we generated *Mrgprd*^{hM3Dq/+};*Mrgprd-Nmb* mice in

which hM3Dq is expressed in NMB-deficient *Mrgprd*⁺ neurons. We found that CNO-induced wiping behavior was not significantly changed in *Mrgprd*^{hM3Dq/+};*Mrgprd-Nmb* mice compared with control *Mrgprd*^{hM3Dq/+} mice (Figure 4I). In contrast, scratching behavior was significantly reduced in *Mrgprd*^{hM3Dq/+};*Mrgprd-Nmb* mice (Figure 4I), substantiating the selectivity of NMB in signaling itch. Taken together, our data demonstrate differential neurotransmitter utilization for pain and itch signaling from *Mrgprd*⁺ neurons. While glutamate is required for the transmission of both pain and itch, NMB is selectively required for transmitting itch but not pain. This provides a mechanism by which *Mrgprd*⁺ neurons code pain and itch signals discretely.

NMB-sensitive spinal neurons postsynaptic to *Mrgprd*⁺ primary afferents are itch selective

Differential neurotransmitter utilization for pain and itch signaling raises the question of whether itch and pain are transmitted by discrete neural circuits. Since NMB is released by *Mrgprd*⁺ neurons to transmit itch signals, we hypothesized that NMB-sensitive neurons postsynaptic to *Mrgprd*⁺ primary afferents selectively process itch signals. To test the hypothesis, we conducted brainstem slice recordings of neurons that express the receptor for NMB (NMBR⁺) in the medullary dorsal horn (MDH). Utilizing *Nmb*^{EGFP} reporter mice,²⁶ we found that β -alanine activation of *Mrgprd*⁺ primary afferents induced depolarization and action potential firings in a subset of *Nmb*^{EGFP+} MDH neurons (Figure 5C), suggesting the synaptic connections between *Mrgprd*⁺ primary afferents and *Nmb*^{EGFP+} MDH neurons. Immunostaining for the presynaptic markers synaptophysin-1 further confirmed that *Mrgprd*⁺ central axons synapse with *Nmb*⁺ neurons (Figure S3).

To determine how glutamate and NMB work together to signal itch, we tested their effects on NMBR⁺ neurons. Electrophysiological recordings of brainstem slices indicated that NMB induced depolarization and action potential firings in *Nmb*^{EGFP+} MDH neurons in a dose-dependent manner (Figures 5A and 5B). In contrast, glutamate (100 μ M) or AMPA (a specific agonist for an ionotropic glutamate receptor, 1 μ M) induced depolarization but failed to induce action potential firings in *Nmb*^{EGFP+} neurons (Figures 5D and 5F). Because the pruritogen β -alanine elicits the release of NMB and low amounts of glutamate from *Mrgprd*⁺ neurons, we further checked how NMB and glutamate work together to signal itch. Remarkably, low-concentration AMPA (1 μ M) significantly potentiated the effects of subthreshold NMB (1 μ M) and induced significant action potential firings of *Nmb*^{EGFP+} MDH neurons (Figures 5D–5F), which was not observed in the control groups treated with AMPA (1 μ M; Figures 5D–5F) or NMB alone (1 μ M; Figure 5B). Our results demonstrate that NMB and glutamate act synergistically on NMBR⁺ central neurons for itch signaling.

To further determine whether NMB-sensitive central neurons transmit itch signals, we ablated NMBR⁺ neurons via intracisternal injection of NMB-saporin (Figure 5G) and examined the consequential behavioral responses to nociceptive stimuli and β -alanine. Paw withdrawal responses to von Frey stimulation and noxious thermal stimuli were not significantly different between neuron-ablated and control mice receiving blank-saporin (Figures 5H–5J). Scratching responses to intradermal β -alanine,

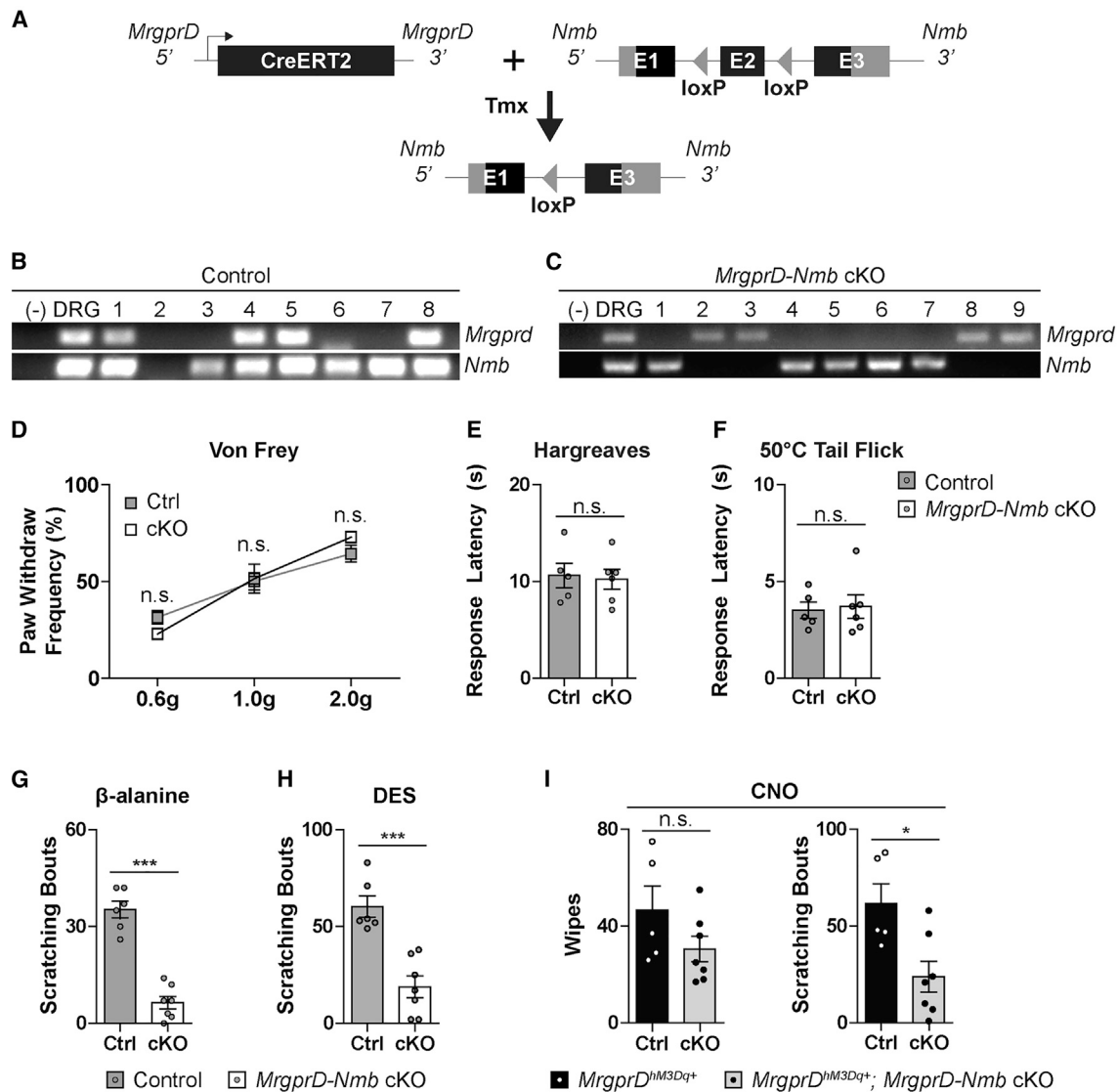


Figure 4. The neuropeptide NMB is selectively required for itch sensation in *MrgprD*⁺ neurons

(A) Breeding strategy for the generation of *MrgprD-Nmb* cKO mice. After tamoxifen-induced cre recombination, the floxed exon 2 of *Nmb*, which encodes the NMB signaling peptide, is excised in *MrgprD*-expressing cells, resulting in the conditional deletion of NMB in *MrgprD*⁺ cells.

(B and C) Single-cell RT-PCR of IB4⁺ DRG neurons from control and *MrgprD-Nmb* cKO mice. After tamoxifen treatment, (B) *Nmb* expression was not affected in DRG neurons from control mice but (C) was undetectable in *MrgprD*⁺ neurons from *MrgprD-Nmb* cKO mice. Note that IB4⁺/*MrgprD*⁻ neurons from both genotypes express *Nmb* (n = 3 mice per genotype).

(D) *MrgprD-Nmb* cKO mice showed similar response frequencies to von Frey stimulation as control littermates (n ≥ 6 per group).

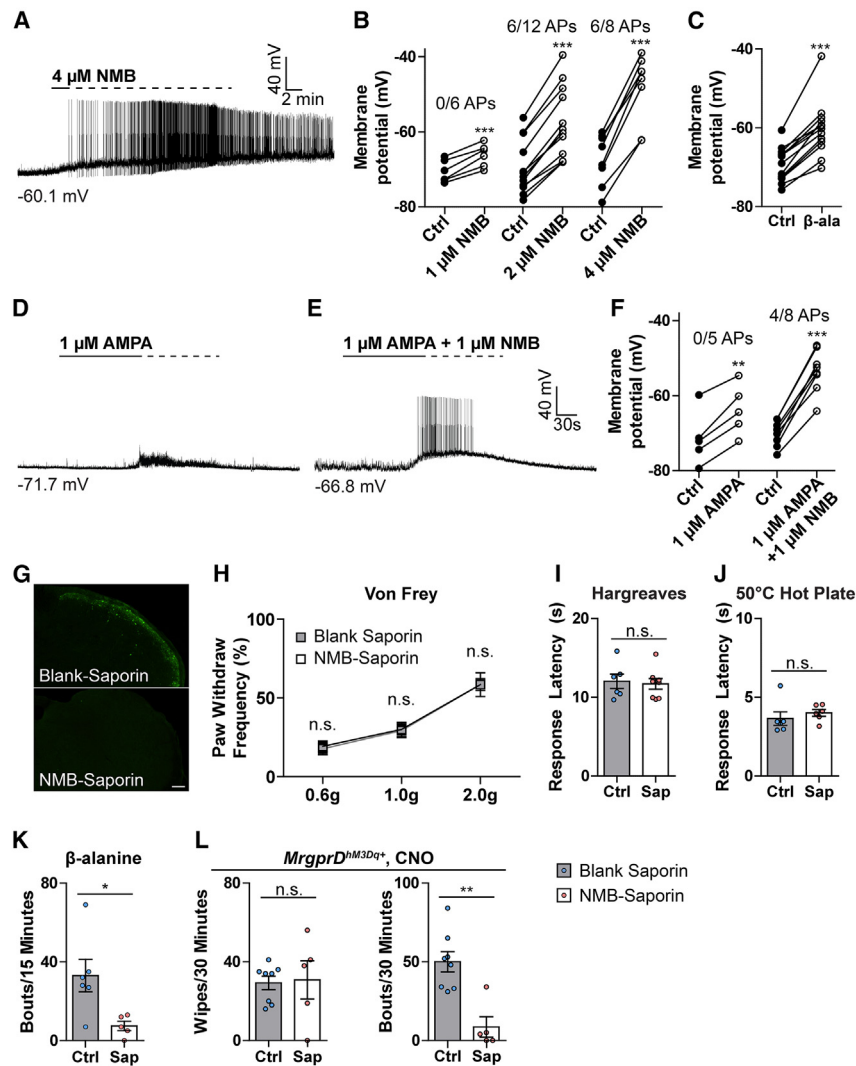
(E and F) *MrgprD-Nmb* cKO mice did not develop defects in thermal nociception, as measured by (E) Hargreaves assay (n ≥ 5 per group) and (F) tail flick assay (50°C, n ≥ 5 per group).

(G and H) β -alanine- (1 μ mol, saline vehicle) (G) and DES (H) (1 μ mol in 50 μ L ethanol vehicle for topical nape application)-induced scratching (bouts/15 min) were significantly reduced (n ≥ 6 per genotype for both experiments).

(I) CNO-induced itch is selectively diminished in *MrgprD*^{hM3Dq/+}; *MrgprD-Nmb* cKO mice. While there was no significant difference in CNO (20 nmol, 1% DMSO saline vehicle)-induced wiping behavior between control and cKO mice, itch-related scratching responses were significantly attenuated in the *MrgprD-Nmb* cKO mice (n ≥ 5 per genotype). Pain and itch behavior was recorded and analyzed for 30 min. Unless otherwise indicated, all injections were 20 μ L at the cheek. Data are presented as mean \pm SEM. Nonparametric Mann-Whitney U tests were used to determine statistical significance for (D)–(I). n.s., no significance. *p \leq 0.05, ***p \leq 0.001.

however, was nearly abolished in neuron-ablated mice (Figure 5K), suggesting that NMB-sensitive postsynaptic neurons are itch selective.

To confirm the selectivity of postsynaptic NMBR⁺ MDH neurons for itch transmission, we ablated NMBR⁺ neurons in *MrgprD*^{hM3Dq/+} mice. CNO-induced pain-related wiping behavior



(L) CNO (20 nmol in 20 μ L cheek, 1% DMSO saline vehicle)-induced wipping responses were not different between blank- or NMB-saporin-injected *MrgprD*^{HM3Dq+} mice, but itch-related scratching was nearly abolished by NMB-saporin injections ($n \geq 5$ mice per group). Pain and itch behavior was recorded and analyzed for 30 min.

Data are presented as mean \pm SEM. Shapiro-Wilk tests were used to determine data normality, and paired (pre/post) Student's *t* tests were used to determine statistical significance for (A), (C), and (F). Nonparametric Mann-Whitney *U* tests were used to determine statistical significance for (H)–(L). * $p \leq 0.05$, ** $p \leq 0.01$, *** $p \leq 0.001$. Scale bars: 50 μ m.

was not significantly changed after NMB-saporin injection (Figure 5L), while itch-related scratching behavior was nearly abolished (Figure 5L). Taken together, our data demonstrate that pain and itch signals from *MrgprD*⁺ neurons are received and processed by NMB-insensitive and NMB-sensitive MDH neurons, respectively, suggesting that discrete MDH populations and central circuits transmit pain and itch signaling from polymodal nociceptive neurons.

DISCUSSION

In this study, we delineated the differential mechanisms for pain and itch coding and transmission from *MrgprD*⁺ polymodal sen-

Figure 5. NMB-sensitive medullary dorsal horn (MDH) neurons receive itch input from *MrgprD*⁺ afferents

(A–F) Ex vivo slice recording of brainstems from *Nmbr*^{EGFP+} mice. (A) Representative whole-cell current-clamp recording of NMB (4 μ M, bath perfusion) response in *Nmbr*^{EGFP+} MDH neurons. (B) Quantification of *Nmbr*^{EGFP+} MDH neuron responses to NMB. NMB dose-dependently induced membrane potential increase in *Nmbr*^{EGFP+} neurons ($n \geq 6$ neurons from 3 mice for each group). (C) β -alanine (1 mM, bath perfusion)-induced increase in membrane potential in a subset of *Nmbr*^{EGFP+} MDH neurons (13/25 neurons, from 10 mice). Synaptic connections were also confirmed by immunostaining; see also Figure S3. (D) Representative whole-cell current-clamp recording of AMPA (1 μ M, bath perfusion). (E) Representative whole-cell current-clamp recording of AMPA and NMB (1 μ M each, bath perfusion). (F) Quantification of *Nmbr*^{EGFP+} MDH neuron responses to AMPA alone and AMPA with NMB. AMPA-enhanced NMB induced membrane potential increase and action potential firing in *Nmbr*^{EGFP+} neurons ($n \geq 5$ neurons from 3 mice for each group). Please note that for (D)–(F), recordings were performed in the presence of 100 μ M picrotoxin and 1 μ M strychnine to block GABA and glycine receptors.

(G) Validation of *Nmbr*^{EGFP+} MDH neuron ablation after intracisternal NMB-saporin injection. GFP signal was found in the MDH of blank-saporin-injected *Nmbr*^{EGFP+} mice. In contrast, no GFP signal was found in the MDH of NMB-saporin-injected *Nmbr*^{EGFP+} mice ($n \geq 3$ mice per group).

(H) Intracisternal NMB-saporin injection did not affect response to von Frey stimulation ($n = 6$ mice per group).

(I and J) Thermal nociception, as measured by (I) Hargreaves assay ($n \geq 6$ per group) and (J) tail flick assay ($n \geq 6$ per group), was not significantly changed by NMB-saporin injection.

(K) Intracisternal NMB-saporin injection attenuated β -alanine (1 μ mol, 20 μ L cheek, saline vehicle)-induced itch-related scratching behavior (bouts/15 min, $n \geq 5$ mice per group).

sory neurons. Our results show that *MrgprD*⁺ neurons utilize two neurotransmitters, glutamate and the neuropeptide NMB, to transmit sensory information. Upon noxious mechanical stimulation, *MrgprD*⁺ neurons release glutamate. By contrast, upon pruritogen challenge, *MrgprD*⁺ neurons release both glutamate (likely in low amounts, as shown in Figure 2G) and NMB to activate an NMB-sensitive, itch-selective central circuit.

As *MrgprD*⁺ polymodal neurons account for ~20% of total sensory neurons,^{9,11} it raises the question of whether *MrgprD*⁺ neurons comprise distinct subsets that mediate pain and itch, respectively. Our and others' studies have shown that pain- and itch-related receptors/ion channels (e.g., *MrgprD*, *Piezo2*) are ubiquitously expressed by *MrgprD*⁺ polymodal neurons,

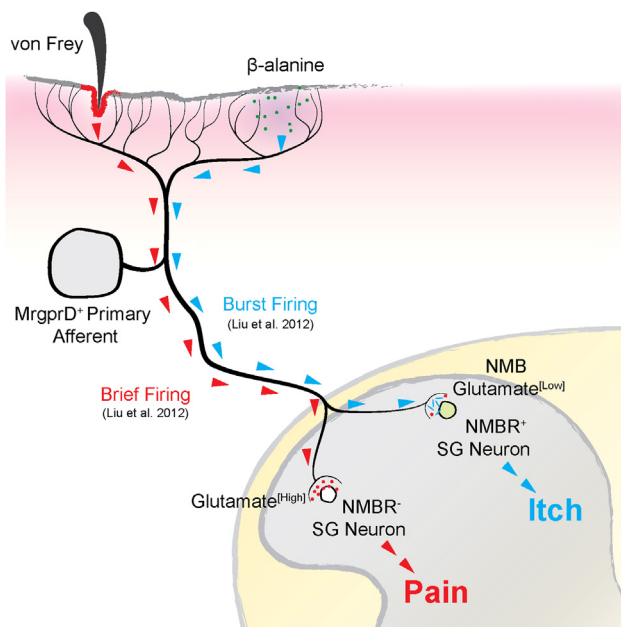


Figure 6. The combinatorial model for pain and itch coding by MrgprD⁺ polymodal neurons

MrgprD⁺ polymodal afferents detect both noxious mechanical forces and pruritic chemical stimuli including β -alanine. Mechanical stimuli induce brief action potential firings in these neurons and glutamate release at their central terminals. In contrast, chemical pruritogens like β -alanine induce burst firings in MrgprD⁺ neurons, which triggers the release of neuropeptide NMB as well as a low level of glutamate release at central terminals. Itch signals are received and processed by NMBR⁺ spinal neurons and related itch pathways.

which enables individual MrgprD⁺ neurons to respond to both itch- and pain-related stimuli.^{6–8} Furthermore, VGlut2 and NMB are broadly expressed by MrgprD⁺ neurons. This suggests that all MrgprD⁺ neurons are capable of releasing pain- and itch-related neurotransmitter(s) to signal distinct neuronal populations in the SG (lamina II) of the spinal cord and brainstem. Therefore, previous and our current studies support the intrinsic polymodality of MrgprD⁺ neurons.

Chemogenetic activation of MrgprD⁺ neurons evokes both pain and itch, correlating well with the polymodality of MrgprD⁺ neurons. Previous study suggested that chemogenetic and optogenetic activation of an itch-selective neuronal population (MrgprA3⁺) generate distinct behavioral consequences (itch vs. pain),²⁷ raising the question of whether these synthetic biology-based approaches unnaturally activate neurons and generate artificial behavioral consequences. Indeed, varying parameters of optogenetic stimulation including light pulse frequency, duration, amplitude (i.e., power), and pattern (e.g., number of pulses in a train, intervals between pulse trains, etc.) activate neurons differentially and result in diverse behavioral consequences.^{17,27,28} Since we have not established the optimal optogenetic stimulation protocol for MrgprD⁺ neurons, this study does not involve optogenetic manipulation of MrgprD⁺ neurons. Instead, we activated MrgprD⁺ neurons using a chemogenetic approach. Our chemogenetic experiment recapitulates the behavioral consequences of activating MrgprD⁺ neurons using

pruritogenic β -alanine and noxious mechanical stimuli, suggesting that chemogenetic stimulation induces genuine intrinsic behavior rather than artificial consequence.

Our previous *in vivo* electrophysiological recordings have shown that noxious mechanical stimulation of MrgprD⁺ neurons induced brief action potential firing, whereas the pruritogen β -alanine induced prolonged burst firing.⁸ While the former firing pattern is sufficient for glutamate release, the latter firing pattern preferentially facilitates the release of neuropeptides.^{29,30} Study has shown that the release of the neuropeptide substance P depends on the number of electrical stimuli and increases with prolonged stimulations.²⁹ Importantly, “stimulation with bursts of three impulses when delivering a fixed number of stimuli resulted in detection of increased levels of substance P.”²⁹ This is comparable to the firing pattern evoked by β -alanine. Interestingly, immunoelectron microscopy (immunoEM) studies indicate that substance P and glutamate are localized in different vesicles (large dense-core vs. small lucent vesicles).³¹ It is very likely that burst firing preferentially facilitates the release of large dense-core vesicles from primary sensory neurons. NMB, as a neuropeptide, may as well be packed in large dense-core vesicles but not glutamate-containing small lucent vesicles. Indeed, our previous and current studies indicate that β -alanine treatments induce prolonged burst firing and elicit a significant release of NMB from MrgprD⁺ neurons. NMB deficiency in MrgprD⁺ neurons selectively abolishes itch but not pain. These results suggest that pain and itch stimuli are detected and encoded into different patterns of electrical activities and neurotransmitter release from MrgprD⁺ neurons (pattern theory).

In the central nervous system, MrgprD⁺ neurons synapse with most known neuronal classes in the SG of the spinal cord and brainstem^{15,16} but have a very limited selection of neurotransmitters (mainly glutamate and NMB) to communicate with SG neurons. The pruritogen β -alanine elicits high NMB release, albeit mild glutamate release, from MrgprD⁺ neurons. Our electrophysiological study further indicates that low amounts of glutamate potentiate the effects of NMB and selectively activate NMBR⁺ SG neurons for itch transmission, which defines a central “labeled line” for itch.

Our finding leads to a working model for MrgprD⁺ polymodal sensory neurons, which comprises the components of both the pattern theory (periphery) and labeled line (central). We name this model “combinatorial coding theory” (Figure 6). In this model, mild glutamate release upon itch stimulation enhances NMB signals to activate the itch pathway while preventing inadvertent activation of pain-processing circuits. In contrast, high glutamate release is required for activating NMB-independent pain pathways and signaling pain. This new model sheds light on the neural mechanism by which polymodal sensory neurons encode and segregate itch and pain signals and advances our understanding of sensory coding and processing in the nervous system.

Limitations of the study

Our study provides insights into the neurotransmitter-based coding mechanisms for pain and itch signals from MrgprD-expressing peripheral afferents. Our experimental methods rely heavily on mouse behavioral models, which result in two main

limitations. First, additional studies are needed to determine whether our described coding mechanism is conserved in other laboratory animals or humans. While *MrgprD* is also expressed by human DRG neurons, the precise level of genetic and functional conservation between human and mouse remains to be determined. Second, additional molecular studies are needed to delineate the mechanisms controlling neurotransmitter release, specifically release of glutamate- vs. neuropeptide-containing synaptic vesicles.

STAR★METHODS

Detailed methods are provided in the online version of this paper and include the following:

- KEY RESOURCES TABLE
- RESOURCE AVAILABILITY
 - Lead contact
 - Materials availability
 - Data and code availability
- EXPERIMENTAL MODEL AND SUBJECT PARTICIPANT DETAILS
- METHOD DETAILS
 - Immunofluorescence
 - *In situ* hybridization
 - Whole-cell patch clamp recordings of dissociated DRG neurons
 - Itch behavioral experiments
 - Pain behavior experiments
 - DRG dissociation and FACS sorting
 - cDNA preparation and RT-PCR
 - Slice preparation and electrophysiological recordings
 - Glutamate and NMB release assay
 - Intracisternal NMB-Saporin injection
- QUANTIFICATION AND STATISTICAL ANALYSIS

SUPPLEMENTAL INFORMATION

Supplemental information can be found online at <https://doi.org/10.1016/j.celrep.2023.113316>.

ACKNOWLEDGMENTS

We would like to thank Dr. Mark Zylka at the University of North School of Medicine for providing *Mrgprd^{EGFP/+}* mutant mice, which were essential to the completion of this study. This work was supported by grants from the NIH to Q.L. (R01EY024704, 1R01AI163146, and 1R01AI125743), the Pew Scholar Award to Q.L., and an NIH R01 grant (NS083702) to W.L.

AUTHOR CONTRIBUTIONS

Conceptualization, C.G., W.L., and Q.L.; methodology, C.G., H.J., W.O., M.F., W.L., and Q.L.; validation, C.G., H.J., C.-C.H., W.L., and Q.L.; formal analysis, C.G., H.J., C.-C.H., and M.F.; investigation, C.G., H.J., C.-C.H., F.L., W.Y., M.F., and G.Y.; resources, C.G., M.F., G.H., W.L., and Q.L.; data curation, C.G., H.J., M.F., W.L., and Q.L.; writing – original draft, C.G. and Q.L.; writing – review & editing, C.G., H.J., G.H., W.L., and Q.L.; visualization, C.G., H.J., W.O., and M.F.; supervision, W.L. and Q.L.; project administration, W.L. and Q.L.; funding acquisition, W.L. and Q.L.

DECLARATION OF INTERESTS

The authors declare no competing interests.

Received: October 4, 2022

Revised: September 5, 2023

Accepted: October 6, 2023

REFERENCES

1. Basbaum, A.I., Bautista, D.M., Scherrer, G., and Julius, D. (2009). Cellular and molecular mechanisms of pain. *Cell* 139, 267–284.
2. Bautista, D.M., Wilson, S.R., and Hoon, M.A. (2014). Why we scratch an itch: the molecules, cells and circuits of itch. *Nat. Neurosci.* 17, 175–182. <https://doi.org/10.1038/nn.3619>.
3. Patel, K.N., and Dong, X. (2011). Itch: Cells, Molecules, and Circuits. *ACS Chem. Neurosci.* 2, 17–25. <https://doi.org/10.1021/cn100085g>.
4. Han, L., Ma, C., Liu, Q., Weng, H.J., Cui, Y., Tang, Z., Kim, Y., Nie, H., Qu, L., Patel, K.N., et al. (2013). A subpopulation of nociceptors specifically linked to itch. *Nat. Neurosci.* 16, 174–182. <https://doi.org/10.1038/nn.3289>.
5. Knowlton, W.M., Palkar, R., Lippoldt, E.K., McCoy, D.D., Baluch, F., Chen, J., and McKerny, D.D. (2013). A sensory-labeled line for cold: TRPM8-expressing sensory neurons define the cellular basis for cold, cold pain, and cooling-mediated analgesia. *J. Neurosci.* 33, 2837–2848. <https://doi.org/10.1523/JNEUROSCI.1943-12.2013>.
6. Dussor, G., Zylka, M.J., Anderson, D.J., and McCleskey, E.W. (2008). Cutaneous sensory neurons expressing the *Mrgprd* receptor sense extracellular ATP and are putative nociceptors. *J. Neurophysiol.* 99, 1581–1589.
7. Rau, K.K., McIlwrath, S.L., Wang, H., Lawson, J.J., Jankowski, M.P., Zylka, M.J., Anderson, D.J., and Koerber, H.R. (2009). *Mrgprd* enhances excitability in specific populations of cutaneous murine polymodal nociceptors. *J. Neurosci.* 29, 8612–8619.
8. Liu, Q., Sikand, P., Ma, C., Tang, Z., Han, L., Li, Z., Sun, S., LaMotte, R.H., and Dong, X. (2012). Mechanisms of itch evoked by beta-alanine. *J. Neurosci.* 32, 14532–14537. <https://doi.org/10.1523/JNEUROSCI.3509-12.2012>.
9. Dong, X., Han, S., Zylka, M.J., Simon, M.I., and Anderson, D.J. (2001). A diverse family of GPCRs expressed in specific subsets of nociceptive sensory neurons. *Cell* 106, 619–632.
10. Zylka, M.J., Dong, X., Southwell, A.L., and Anderson, D.J. (2003). Atypical expansion in mice of the sensory neuron-specific *Mrg G* protein-coupled receptor family. *Proc. Natl. Acad. Sci. USA* 100, 10043–10048. <https://doi.org/10.1073/pnas.1732949100>.
11. Zylka, M.J., Rice, F.L., and Anderson, D.J. (2005). Topographically distinct epidermal nociceptive circuits revealed by axonal tracers targeted to *Mrgprd*. *Neuron* 45, 17–25.
12. Shinohara, T., Harada, M., Ogi, K., Maruyama, M., Fujii, R., Tanaka, H., Fukusumi, S., Komatsu, H., Hosoya, M., Noguchi, Y., et al. (2004). Identification of a G protein-coupled receptor specifically responsive to beta-alanine. *J. Biol. Chem.* 279, 23559–23564.
13. Cavanaugh, D.J., Lee, H., Lo, L., Shields, S.D., Zylka, M.J., Basbaum, A.I., and Anderson, D.J. (2009). Distinct subsets of unmyelinated primary sensory fibers mediate behavioral responses to noxious thermal and mechanical stimuli. *Proc. Natl. Acad. Sci. USA* 106, 9075–9080.
14. Vrontou, S., Wong, A.M., Rau, K.K., Koerber, H.R., and Anderson, D.J. (2013). Genetic identification of C fibres that detect massage-like stroking of hairy skin in vivo. *Nature* 493, 669–673. <https://doi.org/10.1038/nature11810>.
15. Olson, W., Abdus-Saboor, I., Cui, L., Burdige, J., Raabe, T., Ma, M., and Luo, W. (2017). Sparse genetic tracing reveals regionally specific

- functional organization of mammalian nociceptors. *Elife* 6, e29507. <https://doi.org/10.7554/eLife.29507>.
16. Wang, H., and Zylka, M.J. (2009). Mrgprd-expressing polymodal nociceptive neurons innervate most known classes of substantia gelatinosa neurons. *J. Neurosci.* 29, 13202–13209. <https://doi.org/10.1523/JNEUROSCI.3248-09.2009>.
 17. Cui, L., Guo, J., Cranfill, S.L., Gautam, M., Bhattarai, J., Olson, W., Beattie, K., Challis, R.C., Wu, Q., Song, X., et al. (2022). Glutamate in primary afferents is required for itch transmission. *Neuron* 110, 809–823.e5. <https://doi.org/10.1016/j.neuron.2021.12.007>.
 18. Shimada, S.G., and LaMotte, R.H. (2008). Behavioral differentiation between itch and pain in mouse. *Pain* 139, 681–687.
 19. Bai, L., Xu, H., Collins, J.F., and Ghishan, F.K. (2001). Molecular and functional analysis of a novel neuronal vesicular glutamate transporter. *J. Biol. Chem.* 276, 36764–36769. <https://doi.org/10.1074/jbc.M104578200>.
 20. Pogorzala, L.A., Mishra, S.K., and Hoon, M.A. (2013). The cellular code for mammalian thermosensation. *J. Neurosci.* 33, 5533–5541. <https://doi.org/10.1523/JNEUROSCI.5788-12.2013>.
 21. Mishra, S.K., Tisel, S.M., Orestes, P., Bhangoo, S.K., and Hoon, M.A. (2011). TRPV1-lineage neurons are required for thermal sensation. *EMBO J.* 30, 582–593. <https://doi.org/10.1038/emboj.2010.325>.
 22. Lagerström, M.C., Rogoz, K., Abrahamsen, B., Persson, E., Reinius, B., Nordenankar, K., Olund, C., Smith, C., Mendez, J.A., Chen, Z.F., et al. (2010). VGLUT2-dependent sensory neurons in the TRPV1 population regulate pain and itch. *Neuron* 68, 529–542.
 23. Liu, Y., Abdel Samad, O., Zhang, L., Duan, B., Tong, Q., Lopes, C., Ji, R.R., Lowell, B.B., and Ma, Q. (2010). VGLUT2-dependent glutamate release from nociceptors is required to sense pain and suppress itch. *Neuron* 68, 543–556.
 24. Liu, Q., Tang, Z., Surdenikova, L., Kim, S., Patel, K.N., Kim, A., Ru, F., Guan, Y., Weng, H.J., Geng, Y., et al. (2009). Sensory Neuron-Specific GPCR Mrgprs Are Itch Receptors Mediating Chloroquine-Induced Pruritus. *Cell*, 1353–1365.
 25. Uno, M., Nishimura, S., Fukuchi, K., Kaneta, Y., Oda, Y., Komori, H., Takeda, S., Haga, T., Agatsuma, T., and Nara, F. (2012). Identification of physiologically active substances as novel ligands for MRGPRD. *J. Biomed. Biotechnol.* 2012, 816159. <https://doi.org/10.1155/2012/816159>.
 26. Zhao, Z.Q., Wan, L., Liu, X.Y., Huo, F.Q., Li, H., Barry, D.M., Krieger, S., Kim, S., Liu, Z.C., Xu, J., et al. (2014). Cross-inhibition of NMBR and GRPR signaling maintains normal histaminergic itch transmission. *J. Neurosci.* 34, 12402–12414. <https://doi.org/10.1523/JNEUROSCI.1709-14.2014>.
 27. Sharif, B., Ase, A.R., Ribeiro-da-Silva, A., and Séguéla, P. (2020). Differential Coding of Itch and Pain by a Subpopulation of Primary Afferent Neurons. *Neuron* 106, 940–951.e4. <https://doi.org/10.1016/j.neuron.2020.03.021>.
 28. Sun, S., Xu, Q., Guo, C., Guan, Y., Liu, Q., and Dong, X. (2017). Leaky Gate Model: Intensity-Dependent Coding of Pain and Itch in the Spinal Cord. *Neuron* 93, 840–853.e5. <https://doi.org/10.1016/j.neuron.2017.01.012>.
 29. Duggan, A.W., Riley, R.C., Mark, M.A., MacMillan, S.J., and Schaible, H.G. (1995). Afferent volley patterns and the spinal release of immunoreactive substance P in the dorsal horn of the anaesthetized spinal cat. *Neuroscience* 65, 849–858.
 30. Svensson, E., Apergis-Schoute, J., Burnstock, G., Nusbaum, M.P., Parker, D., and Schiöth, H.B. (2018). General Principles of Neuronal Co-transmission: Insights From Multiple Model Systems. *Front. Neural Circuits* 12, 117. <https://doi.org/10.3389/fncir.2018.00117>.
 31. Kandel, E.R., Schwartz, J.H., and Jessell, T.M. (2000). *Principles of Neural Science*, 4th edition (McGraw-Hill), p. 476.
 32. Fleming, M.S., Vysochan, A., Paixão, S., Niu, J., Klein, R., Savitt, J.M., and Luo, W. (2015). Cis and trans RET signaling control the survival and central projection growth of rapidly adapting mechanoreceptors. *Elife* 4, e06828. <https://doi.org/10.7554/eLife.06828>.
 33. Huang, C.C., Yang, W., Guo, C., Jiang, H., Li, F., Xiao, M., Davidson, S., Yu, G., Duan, B., Huang, T., et al. (2018). Anatomical and functional dichotomy of ocular itch and pain. *Nat. Med.* 24, 1268–1276. <https://doi.org/10.1038/s41591-018-0083-x>.

STAR★METHODS

KEY RESOURCES TABLE

REAGENT or RESOURCE	SOURCE	IDENTIFIER
Antibodies		
rabbit anti-GFP	Life Tech	Cat# A11122; RRID: AB_221569
chicken anti-GFP	Aves	Cat# GFP-1020; RRID: AB_2307313
Alexa Fluor 488 conjugated IB4	Life Tech	Cat# I21411
guinea pig anti-Vglut2	EMD	Cat# AB2251
guinea pig anti-Synaptophysin 1	Synaptic Systems	Cat# 101-004
donkey anti-chicken AF488 conjugated	Jackson ImmunoResearch	Cat# 703-546-155; RRID: AB_2340376
donkey anti-guinea pig Cy3 conjugated	Jackson ImmunoResearch	Cat# 706-165-148; RRID: AB_2340460
donkey anti-guinea pig AF647 conjugated	Jackson ImmunoResearch	Cat# 706-605-148; RRID: AB_2340476
goat anti-rabbit AF488 conjugated	Molecular Probes	Cat# A-11034; RRID: AB_2576217
sheep anti-Digoxigenin-AP, Fab fragments	Roche	Cat# 11093274910
sheep anti-Fluorescein-POD, Fab fragments	Roche	Cat# 11426346910
Chemicals, peptides, and recombinant proteins		
Neuromedin B (porcine)	Tocris	Cat# 1908
ISH BLocking Reagent	Roche	Cat# 11096176001
Fluoromount-G	Southern Biotech	Cat# 0100-01
OPAL 520 REAGENT PACK	Akoya Biosciences	Cat# FP1487001KT
OPAL 570 REAGENT PACK	Akoya Biosciences	Cat# FP1488001KT
Clozapine-N-Oxide	Tocris	Cat# 4936
Diethylstilbestrol	Sigma	Cat# D4628-1G
NMB-Saporin KIT	KIT-70	Advanced Targeting Systems
Critical commercial assays		
Glutamate Assay Kit	Sigma	Cat# MAK004
Mouse NMB/Neuromedin B (Competitive EIA) ELISA Kit	LSBio	Cat# LS-F4262-1
TSA Plus system	Perkin Elmer	Cat# NEL741001KT
HNPP Fluorescent Detection Set	Roche	Cat# 11758888001
RNAScope Multiplex Fluorescent V2 Assay	Advanced Cell Diagnostics	Cat# 323110
RNeasy Mini Kit	Qiagen	Cat# 74104
First-Strand Enzyme Kit	New England Biolabs	Cat# E6300S
Taq DNA Polymerase kit	New England Biolabs	Cat# E5000S
SuperScript III CellsDirect cDNA Synthesis kit	Invitrogen	Cat# 18080200
HotStar Taq Polymerase	Qiagen	Cat# 203203
Experimental models: Organisms/strains		
<i>Mrgprd^{tm1.1(Cre/ERT2)Wql}</i>	Penn Gene Targeting Core and Laboratory	N/A
<i>C57BL/6J</i>	The Jackson Laboratory	Stock# 000664
<i>Rosa^{tm14(CAG-tdTomato)Hze/J}</i>	The Jackson Laboratory	Stock# 007908
<i>Tg(CAG-Chrm3*, -mCitrine)Ute/J</i>	The Jackson Laboratory	Stock# 026220
<i>Slc17a6^{tm1Low/J}</i>	The Jackson Laboratory	Stock# 012898
<i>NMB^{tm1.1(KOMP)Vlcg/J}</i>	The Jackson Laboratory	Stock# 025862
<i>Mrgprd^{EGFPf}</i>	Dr. Mark Zylka, the University of North Carolina at Chapel Hill	N/A
<i>Nmb^{EGFP}</i>	Dr. Zhou-feng Chen, Washington University in St. Louis	N/A
Oligonucleotides		
Oligonucleotides	This paper	Tables S1 and S2

(Continued on next page)

Continued

REAGENT or RESOURCE	SOURCE	IDENTIFIER
Software and algorithms		
Graphpad Prism V	Graphpad	N/A
pClamp 10.5	Molecular Devices	N/A
Other		
Mm-Mrgprd probe	Advanced Cell Diagnostics	Cat# 417921
CHRM3-No-XMm-O1-C2 Probe	Advanced Cell Diagnostics	Cat# 1071861-C2
Glass Bottomed Dishes	MatTek	Cat# P35G-0-7-C
SMARTouch controller	World Precision Instruments	Cat# 40220
Vibratome Series 3000 Plus Tissue Sectioning System	Leica Instruments	N/A
MultiClamp 700B amplifier	Molecular Devices	N/A

RESOURCE AVAILABILITY

Lead contact

Further information and requests for resources and reagents should be directed to and will be fulfilled by the lead contact and corresponding author, Qin Liu (qinliu@wustl.edu).

Materials availability

This study did not generate new reagents.

Data and code availability

- The presented data is available from the [lead contact](#) upon request.
- This study did not generate new code.
- Any additional information required to reanalyze the data reported in this work paper is available from the [lead contact](#) upon request.

EXPERIMENTAL MODEL AND SUBJECT PARTICIPANT DETAILS

Mrgprd^{tm1.1(cre/ERT2)Wql} was generated by Penn Gene Targeting Core and Laboratory (PGT), University of Pennsylvania. Cre recombination in experimental mice were induced in mice postnatally (P28) with tamoxifen.

C57BL/6J wild-type (Stock#: 000664), *Rosa*^{tm14(CAG-tdTomato)Hze/J} (Stock#: 007908), *Tg(CAG-Chrm3*, -mCitrine)Ute/J* (Stock#: 026220), *Slc17a6*^{tm1Lowl/J} (Stock#: 012898), and *NMB*^{tm1.1(KOMP)Vlclg/J} (Stock#: 025862) mice were purchased from the Jackson Laboratory. *Mrgprd*^{EGFP} knock-in mice were gifted by Dr. Mark Zylka at the University of North Carolina at Chapel Hill in Chapel Hill, North Carolina. *Nmb*^{EGFP} mice were from Dr. Zhou-Feng Chen when he worked at Washington University School of Medicine in St. Louis. All animals were bred and housed in pathogen free vivarium with 12 h light:dark and 72°F–74°F temperature control until the start of experiments. For all behavioral experiments, researchers were blinded to mouse genotype throughout experimentation and analysis, and animal testing order was assigned by simple randomization. Mixed gender animals were used when possible. All experiments were performed according to National Institutes of Health guidelines and protocols approved by the Institutional Animal Care and Use Committees of Washington University in St. Louis School of Medicine and that of the University of Pennsylvania.

METHOD DETAILS

Immunofluorescence

Adult 8- to 10-week-old mice were anesthetized with ketamine/xylazine cocktail and perfused with 20 mL of ice-cold phosphate buffer solution (PBS, pH 7.4) followed by 45 mL of ice-cold fixative (4% paraformaldehyde (PFA) in PBS). Trigeminal ganglia (TG) and dorsal root ganglia (DRG) were dissected and post-fixed in ice-cold fixative for 20 min. After post-fixation, dissected tissues were placed into a 20% sucrose (w/v) in PBS solution for 24 h for cyroprotection, frozen in OCT, and sectioned at 10 or 20 μm using a Leica CM1950 cryostat. Sections were dried at ambient temperature for 2 h before use.

Sections were washed using 0.1% Triton X-100 in PBS (PBST) and incubated in a blocking solution (10% normal goat serum (NGS) in PBST) for 1 h. After blocking, sections were incubated in the primary antibodies (diluted in 1% NGS in PBST) overnight at 4°C. Sections were washed the following morning with PBST and incubated in fluorescent conjugated secondary antibodies (diluted in 1% NGS in PBST) at ambient temperature for 2 h. Slides were then washed using PBST, mounted, and allowed to dry overnight before imaging.

The following antibodies and dyes were used: rabbit anti-GFP (Life Tech, A11122), chicken anti-GFP (Aves, GFP-1020), Alexa Fluor 488 conjugated IB4 (LifeTech, I21411), guinea pig anti-Vglut2 (EMD, AB2251), guinea pig anti-Synaptophysin 1 (Synaptic Systems, 101-004), donkey anti-chicken AF488 conjugated (Jackson ImmunoResearch, 703-546-155), donkey anti-guinea pig Cy3 conjugated (Jackson ImmunoResearch, 706-165-148), donkey anti-guinea pig AF647 conjugated (Jackson ImmunoResearch, 706-605-148), and goat anti-rabbit AF488 conjugated (Molecular Probes, A-11034). tdTomato and mCitrine fluorescence were visualized directly.

In situ hybridization

ISH procedure was adapted from a previous study.³² Slides were washed in freshly prepared DEPC PBS (1:1000 DEPC in PBS immediately before use), followed by wash in DEPC-pretreated PBS (1:1000 DEPC in PBS overnight, followed by autoclaving). Sections were immersed in freshly boiled antigen retrieval solution (10 mM citric acid, 0.05% Tween 20, pH = 6.0 with 1:1000 diluted DEPC) in a 95°C water bath for 20 min and then allowed to cool at room temperature for 30 min. Sections were washed in DEPC pretreated PBS, incubated in Proteinase K (25 µg/mL in DEPC-pretreated H₂O) for 5 min and washed in fresh-DEPC PBS and DEPC pre-treated PBS. Sections were then incubated in freshly made acetylation solution (0.1 M triethanolamine, 0.25% acetic anhydride in DEPC pretreated H₂O) for 10 min at room temperature. Next, slides were prehybridized in hybridization buffer (50% formamide, 5XSSC, 0.3 mg/mL yeast tRNA, 100 µg/mL heparin, 1X Denhardt's, 0.1% Tween 20, 0.1% CHAPS, 5 mM EDTA in RNase free H₂O) at 62°C in a humidified chamber for 30 min. Following prehybridization, 1–2 ng/µL each of DIG and FITC labeled riboprobe (for double probe *in situ*) diluted in hybridization buffer was placed on the slide. Slides were incubated overnight under Parafilm coverslips at 62°C and then washed in 0.2X SSC at 68°C.

For double probe ISH, following hybridization, slides were blocked for 1 h at room temperature with 0.5% Blocking Reagent (Roche, 11096176001) in PBS. Sections were incubated in anti-FITC-POD (Roche, 11426346910; 1:100 in .5% Blocking Reagent) O/N at 4°C. Slides were then washed in PBT and incubated in 0.1% BSA in PBS for 15 min. FITC riboprobes were then developed using the TSA Plus system (PerkinElmer, NEL741001KT) by diluting fluorescein tyramide into 1X amplification buffer (1:100) and incubating slides in working solution for 10–15 min, followed by washes in PBS. Slides were then blocked in 20% lamb serum in PBT for 1 h at room temperature and incubated overnight at 4°C with alkaline phosphatase(AP)-conjugated anti-DIG antibody (Roche, 11093274910; 1:500 in PBT +20% lamb serum). Slides were washed in TNT (100mM Tris-HCl, 150mM NaCl, 0.05% Tween 20, pH7.5) (3 × 10 min) then in detection buffer (100mM Tris-HCl, 100mM NaCl, 10mM MgCl₂, pH8.0) (2 × 10 min). DIG-labeled riboprobes were then developed using HNPP/Fast Red TR system (Roche, 11758888001). Sections were incubated in detection solution (10 µL HNPP stock solution, 10 µL of 25 mg/mL FastRed per mL of detection buffer, filtered through 0.2µM nylon filter) (3 × 30 min), with TNT rinses between incubations. Slides were then washed in PBS (3 × 10 min) and mounted with Fluoromount-G (Southern Biotech, 0100-01). The probes used are listed in Table S1.

Fluorescent multiplex RNAScope staining was performed using a procedure adapted from the manufacturer's recommended protocol. Animals were sacrificed using carbon dioxide asphyxiation and transcardially perfused with ice-cold PBS to quickly lower body temperature. DRG and TG tissues were dissected, embedded in OCT, immediately sectioned at 20 µm using a cryostat, and slide mounted. Slides were allowed to dry for 1 h in a frost free –20°C freezer. After drying, tissue sections were fixed in ice-cold 4% PFA for 15 min and washed in PBS. Samples were then processed and stained as recommended by the manufacturer. Probes used were Mm-Mrgprd (417921) and Hs-CHRM3-No-XMm-O1-C2 (1071861-C2), both from Advanced Cell Diagnostics, Inc. Signal was developed using the RNAScope Multiplex Fluorescent Detection Reagents V2 (ACD, 323110) and Opal 520 and 570 fluorophore reagents (Akoya Biosciences, FP1487001KT and FP1488001KT respectively). After staining, slides were mounted using DAPI Fluoromount-G (SouthernBiotech, 0100-20), dried at 4°C overnight before imaging. Total processing time between animal sacrifice and mounting was less than 28 h.

Whole-cell patch clamp recordings of dissociated DRG neurons

DRGs were dissected from adult, tamoxifen treated *Mrgprd*^{hM3Dq/+} and control mice. Dissected DRGs were dissociated with dispase (4U/ml) and collagenase (342 U/ml). DRG neurons were then purified using a protocol adapted from our previous study.³³ Specifically, 200 µL of cell suspension was loaded onto 1.2 mL of 15% (w/v) bovine serum albumin in a microcentrifuge tube and centrifuged at 350g for 5 min. After centrifugation, the supernatant was discarded and the pellet of purified neurons was collected.

Dissociated DRG neurons were first incubated with 5 µg/mL isolectin GS-IB4 conjugated to Alexa Fluor 488 (Molecular Probes, I21411) for 10 min and washed with external solution containing (in mM): NaCl 145, KCl 3, CaCl₂ 2, MgCl₂ 2, glucose 10 and HEPES 10, pH 7.4. Only neurons stained with a fluorescent ring around the perimeter of the soma were considered as IB4-positive neurons (IB4⁺). Whole-cell current-clamp recordings were performed using a MultiClamp 700B amplifier and pCLAMP 10.5 software (Axon Instruments). The patch pipettes were pulled from borosilicate glass capillaries (World Precision Instruments) with a P97 horizontal puller (Sutter Instrument). The resistance of the patch pipettes was 3–5 MΩ after filled with an internal solution, the liquid junction potentials were corrected, and the series resistance was routinely compensated at 60%–80%. Internal solution contained (in mM): K⁺-gluconate 120, KCl 30, MgCl₂ 2, HEPES 10, MgATP 2, CaCl₂ 1, EGTA 11, with pH adjusted to 7.2 using Tris-base. Coverslip with neurons were placed in a recording chamber and continuously perfused (~2.5 mL/min) with external solution. Resting membrane potential (RMP) was recorded after stabilization and unhealthy neurons (with RMP > –45 mV) were excluded from the study.

Itch behavioral experiments

All behavioral tests were performed as previously described.^{8,24} In short, 8 to 10-week-old male transgenic mice, along with *wild-type* or control littermates, were given intradermal injection of vehicle, Clozapine-N-Oxide (1 mM in 1% DMSO saline), or pruritic compounds into the cheek. Test animals were then placed alone into their testing chamber and video recorded for 15 to 30 min. Video tapes were played back after the completion of the experiment and scratches with the hind paw and wipes with the fore limb directed at the injection site were scored. For the measurement of spontaneous itch, mice of the indicated age were acclimated in the testing chambers the day before testing and filmed for 30 min on the day of the test. All scratching bouts were scored.

In the DES model, test animals were shaved at the rostral back. Starting three days after shaving, an 1:1 acetone:diethylether solution (Sigma) was applied onto the shaved area using a 1 cm × 1.5 cm cotton pad for 15 s twice daily for four consecutive days to disrupt the skin barrier at the treatment site, and allow greater compound penetration on the day of testing. Test animals do not develop appreciable spontaneous itching before the start of the experiment. In the morning after the final treatment, a 50 μ L ethanol vehicle was applied topically at the test site of treated animals using a 200 μ L pipettor and videoed for 30 min. Test animals were allowed to recover for an additional 30 min before 50 μ L of 20 mM DES solution was applied at the treated site. Animals were videoed for 30 min again. Scratch bouts directed at the treated site were scored afterward.

Pain behavior experiments

Pain behavioral tests were conducted as previously described.^{4,24} In the von Frey assays, mice were placed into acrylic behavioral chambers on a metal mesh. Von Frey filaments, each applying a specific force, were applied to the underside of the paw until bending. Each filament was kept in place for 3 s before removal. Animals were allowed to recover for 5 min between tests and were tested 10 times with each filament. Frequency of paw withdraw to each weight filament was scored.

Hargreaves Assays were conducted using a purpose-built testing apparatus from IITC. Briefly, mice were placed into acrylic behavioral chambers on a heated (30°C) glass plate and radiating heat (Active Intensity set to 15%) was applied to the underside of the paw until pain-related responses, i.e., paw withdraw, shaking or licking, was observed. Animals were allowed to recover for 20 min between tests. Latency between stimuli application and behavioral response was scored, and an average response latency was calculated for each mouse based on the results of 3 repeats.

Tail flick assays were conducted using a custom-built restraining device and a water bath preheated to 50°C. Animals were restrained so that their tails are completely exposed with unrestricted movement, while the rest of the body was immobilized. During each test, 3 inches of tail was submerged into the water bath until pain-related responses, i.e., vigorous tail flicking, was observed. After each test, animals were removed from the restraining device and were allowed to recover for 20 min between tests. Latency between stimuli application and behavioral response was scored, and an average response latency was calculated for each mouse based on the results of 3 repeats.

DRG dissociation and FACS sorting

~150 dorsal root ganglia were dissected on ice from three 8-weeks old *Mrgprd*^{EGFP+} mice, along with ~50 ganglia from an age-matched *wild-type* control mouse, were dissected on ice and processed individually. Dissected DRGs were dissociated using a 4 U/ml dispase/342 U/ml collagenase Type I mixture in HBSS at 37°C for 30 min with constant, gentle agitation. After dissociation, the enzyme mix was removed and replaced with DMEM/F12 media supplemented with 10% FBS and 1% Penicillin/streptomycin antibiotic mix. DRGs were then gently triturated using a 1 mL pipettor to break apart the ganglia and suspend the cells. Triturated cells were filtered through a 70 μ m cell strainer to remove large debris and pooled in a 15 mL conical bottomed tube and centrifuged at 300g for 4 min to pellet the cells. After centrifugation, media was aspirated from the cell pellet and the pellet was resuspended in 200 μ L of fresh media. Cell suspensions from each mouse were then divided into two equal 100 μ L parts. Each part was gently transferred and layered onto the top off 2 mL of freshly prepared 15% (w/v) bovine serum albumin/sterile HBSS solution in 15 mL conical tube. The tubes were then centrifuged at 350g for 4 min to separate DRG neurons from axonal debris and glia. After centrifugation, purified neurons formed pellets on the bottom of the tubes. The supernatant was gently aspirated and DRG neurons from each genotype were resuspended and pooled into 200 μ L total of FACS sorting buffer (2% FBS in sterile PBS) and filtered through a 40 μ m strainer to remove any remaining large debris. The GFP expressing fraction of the purified DRGs was then isolated into fresh media using a BD FACS Aria II sorter and previously reported settings (Chiu et al., 2014). DRG neurons from the wild-type mouse served as the negative control for GFP fluorescence during sorting.

cDNA preparation and RT-PCR

Freshly isolated *Mrgprd*^{EGFP+} neurons (~36,000 *Mrgprd*^{EGFP+} neurons were collected) were centrifuged at 400g for 4 min to pellet the cells. Media was then removed, and the pellet was gently washed once with HBSS. mRNA from isolated cells were purified, and cDNA library were compiled using First-Strand enzyme Kit (NEB, E6300S) and PCR was performed using the Taq DNA Polymerase kit (NEB, E5000S) using the manufacturer's recommended protocols. PCR was run using 60°C annealing for 40 cycles.

For single cell RT-PCR, adherent culture DRG neurons were picked by hand using a Leica widefield microscope and Warner 3-axis micromanipulator. cDNA library was generated using the Invitrogen SuperScript III CellsDirect cDNA Synthesis Kit (Life Tech, 18080200) and RT-PCR was performed using the HotStar Taq Polymerase (Qiagen, 203203). PCR was run using 60°C annealing for 50 cycles. Primer sequences used are listed in Table S2.

Slice preparation and electrophysiological recordings

Male mice (P14-P21) were deeply anesthetized with isoflurane and decapitated at the cervical spinal level. The brainstem was removed in an ice-cold oxygenated (95% O₂, 5% CO₂) sucrose-based solution containing (in mM): Sucrose 209, KCl 2, NaH₂PO₄ 1.25, MgCl₂ 5, CaCl₂ 0.5, NaHCO₃ 26 and glucose 10. The brainstem was vertically embedded in agar with its rostral end up and serial transverse brainstem slices (350 μm thick) were made from caudal to rostral using a vibrating tissue slicer (Vibratome 3000 Plus). Slices were allowed to recover at 34°C for 30min in holding artificial cerebrospinal fluid (ACSF) containing (in mM): NaCl 92, KCl 2.5, NaH₂PO₄ 1.25, NaHCO₃ 30, MgCl₂ 2, CaCl₂ 2, glucose 25 and HEPES 20, saturated with 95% O₂, 5% CO₂. Following recovery, slices were placed at room temperature for 1h prior to recording.

After incubation, slices were placed in a recording chamber continuously superfused with oxygenated recording ACSF containing (in mM): NaCl 124, KCl 2.5, NaH₂PO₄ 1.25, NaHCO₃ 24, MgCl₂ 1, CaCl₂ 2, glucose 12.5 and HEPES 5, at a rate of ~2.5 mL/min at room temperature. Whole-cell current-clamp recordings were performed on Nmb^{rGFP+} MDH neurons of brainstem slices using a MultiClamp 700B amplifier and pCLAMP 10.5 software (Axon Instruments). Neurons were visualized by fluorescence to identify fluorescent protein positive neurons followed by infrared differential interference contrast microscopy for placing of the patch pipette. The resistance of the patch pipettes was 5–8 MΩ after filled with an internal solution, the liquid junction potentials were corrected and the series resistance was routinely compensated at 60%–80%. The internal solution contained the following (in mM): K⁺-gluconate 130, NaCl 10, MgCl₂ 1, EGTA 0.2, HEPES10, Mg-ATP 1, Na-GTP 5 with an osmolarity of 290–300 mOsm and a pH that was adjusted to 7.25 using KOH.

Glutamate and NMB release assay

To determine neurotransmitter release from MrgprD⁺ neurons after stimulation, DRG neurons were dissected from *Mrgprd*^{hM3Dq/+} and control littermates, dissociated using dispase/collagenase enzyme mixture, and purified using 15% BSA as previously described. Afterward, the purified neurons were seeded onto recessed glass windows of Poly-D-Lysine (Corning, 354210) coated glass bottomed dishes (MatTek, P35G-0-7-C), and cultured for 36 h before use. Before the experiment, culture media was gently aspirated and neurons were washed using prewarmed, 37°C CIB. After wash, 50 μL of warm CIB was then slowly and gently pipetted onto the neurons and collected after 60s as the vehicle control. Extreme care was taken during pipetting to avoid mechanical stimulation of the cultured neurons and to avoid rupturing or detaching the cultured neurons. The same volume of 500 μM CNO or 1 mM β-alanine was then pipetted onto the neurons and collected using the same procedure. The collected supernatants were flash frozen and stored at –80°C until assay. Culture media was then replaced, and neurons were cultured for an additional 6 h before treatment with the positive control, 30 mM KCl.

Glutamate concentration was determined by colorimetric assay using a Glutamate Assay Kit (Sigma, MAK004) and NMB concentration was determined by ELISA using a Mouse NMB Kit (LSBio, LS-F4262-1). Calculated neurotransmitter concentrations were corrected for all dilutions performed for the assays, and normalized to that of the vehicle controls.

Intracisternal NMB-Saporin injection

To ablate NMB sensitive neurons in the brain stem, 5-week-old C57BL/6J mice were anesthetized using a ketamine/xyzazine cocktail (Putney, B4N4). After loss of toe pinch reflex, animals were placed in a custom-made restrainer and the head was immobilized at a slightly downward angle to expose the cleft between the occiput and atlas vertebrae. A 30-gauged needle syringe, with 30° bend approximately 2.5 mm down from the point of the bevel, was inserted into the cleft and 3 μg of NMB-Saporin (Advanced Targeting Systems, IT-70-25), dissolved in 5 μL of saline was injected into the mouse. The NMB-saporin injection was repeated 48 h later. Control mice were injected with unconjugated saporin (blank-saporin) or saline vehicle. Three weeks after the second injection, animals were used for behavioral experiments.

QUANTIFICATION AND STATISTICAL ANALYSIS

Sample sizes were chosen based on recently published papers that are relevant to our study. Itch behavior was scored using videotapes by observers blinded to mouse genotypes. Quantification of overlap in immunofluorescence and *in situ* hybridization experiments was determined based on images from at least three mice, with 3–5 sections per animal. Graphs were generated and statistical significances for all mouse behavioral experiments were determined using nonparametric Mann Whitney U tests. For all other datasets, Shapiro-Wilk tests were performed to confirm normality, followed by student's *t* tests to determine statistical significance. Paired testing was performed for data that used pre/post measurements, specifically Figure 2, panels G-H, and Figure 5, panels A, C, and F. Unpaired tests were used for all other relevant panels. Statistical analysis was performed and graphs were generated using Graphpad Prism V (Graphpad, La Jolla, CA). All data is presented as mean ± standard error of the mean (SEM). Differences were considered significant if *p* ≤ 0.05.